VARIATIONAL BELTRAMI FLOWS OVER MANIFOLDS

Nir Sochen [*]

Dept. of Applied Mathematics
University of Tel-Aviv
Ramat-Aviv, tel-Aviv 69978, Israel
sochen@math.tau.ac.il

Rachid Deriche and Lucero Lopez-Perez

Odysee Laboratoire
INRIA Sophia-Antipolis
2004 Route des Lucioles
06902 Sophia-Antipolis CEDEX, France
Rachid.Deriche@sophia.inria.fr
Lucero.Lopez_perez@sophia.inria.fr

ABSTRACT

We study, in this paper, the problem of denoising images/data which are defined over non-flat surfaces. This problem arises often in many medical imaging tasks. The Beltrami flow which was defined in an explicit-intrinsic manner is generalized here to non-flat surfaces and is defined in an implicit way. We formulate the flow in a variational way which is generalized to a scalar field defined over an n-dimensional manifold. The implementation scheme of this flow is presented and various experimental results obtained on a set of real images illustrate the performances of the approach as well as the differences between various flows of interests.

1. INTRODUCTION

It was realized in recent years that powerful techniques, that were devised to denoise and regularize various objects such as intensity, color and various vector fields on flat space, need to be generalized to non-flat domains. This is typical in many medical imaging processes were the relevant data is attached to a specific tissue such as the colon or the cortex.

Two approaches for regularizing an image on a non-flat surface are known. The Beltrami [19, 20, 22, 10, 18] and the harmonic map [3, 14, 6, 4, 17] frameworks define, both, the regularization as a gradient descent flow of a geometric functional[1]. It has been shown, in various works [14, 1], that these two functionals are in fact the same. The surface is expressed in the harmonic map formulation in an implicit way and in the Beltrami framework in an explicit-intrinsic manner. Yet, the denoising flows, obtained in these two formulations, defer because of different formulations of the problem in the two frameworks. We explain in the present study the differences in the formulation of the problem and generalize, subsequently, the Beltrami flow to non-flat manifolds. We generalize, via the variational approach, our previous results [2] where the Beltrami flow was derived for a scalar field defined over a curve. In [2] the derivation was purely geometric and limited, therefore to the one-dimensional case.

In order to explain the frameworks we have to describe the space in which these functionals operate. Many of the problems in image processing and computer vision are approached by the attachment of a feature space to every point (or pixel in the discrete setting). The feature spaces in different locations of the image domain are isomorphic. The combined spatial-feature space is called a fiber bundle. The image domain is called the base manifold and the feature space is called the fiber. If the feature space is a vector space then the spatial-feature space is called a vector bundle. The choice of a point in the feature space to any point in the image domain (the base manifold) is called a section.

In the harmonic map formulation the functional evaluates the embedding of **the base manifold** in the fiber. The Polyakov action in the Beltrami framework evaluates the embedding of **the section** in the spatial-feature space (the fiber bundle). We will see below that this difference leads to different denoising flows.

This article is organized as follows: The Beltrami intrinsic approach is used in Section 2 to derive equations for the denoising of gray value images defined over a flat 2D surfaces. We take in Section 3 the Beltrami formulation of scalar denoising on non-flat manifold and reformulate it in an implicit form. The derived implicit equation, obtained in section 4, is the gradient descent equation for the functional. Section 5 presents examples and results.

2. INTRINSIC FORMULATION

Suppose we have a 2-dimensional manifold Σ with local coordinates σ^1, σ^2 embedded in an 3-dimensional manifold M with coordinates X^1, X^2, X^3, the embedding map $X : \Sigma \to M$ is given explicitly by the 3 functions of 2 variables

$$X : (\sigma^1, \sigma^2) \longrightarrow (X^1(\sigma^1, \sigma^2), X^2(\sigma^1, \sigma^2), X^3(\sigma^1, \sigma^2)) .$$

A gray-value image $U(\sigma^1, \sigma^2)$ is represented, in this framework, as the embedding $(X^1 = \sigma^1, X^2 = \sigma^2, X^3 = \beta U(\sigma^1, \sigma^2))$.

Let us formulate the Polyakov action [15] in a matricial form: Let (Σ, G) be the image manifold and its metric and (M, H) the spatial-feature manifold and its metric. The spatial-feature manifold M is simply $\mathbb{R}^3$ with the usual Eucledean distance for gray-value images. Define at each point the matrix A whose elements are

$$A^{ij} = (\partial_\Sigma X^i)^t G^{-1} \partial_\Sigma X^j ,$$

where $\partial_\Sigma X^i = (\partial_{\sigma^1} X^i, \partial_{\sigma^2} X^i)^t$.

The map $X : \Sigma \to M$ has the following weight:

$$S[X^i, G, H] = \int d^m \sigma \sqrt{g} \mathrm{Tr}(AH),$$

---

[1]For geometric non-variational approach, see [9]

where m is the dimension of Σ and $g = \det(G)$.

The gradient descent equations, with respect to X^3 in our gray-level image example is

$$U_t = -\frac{1}{2\sqrt{g}}\frac{\delta S}{\delta U} = \underbrace{\frac{1}{\sqrt{g}}\mathrm{div}\left(\sqrt{g}G^{-1}\nabla U\right)}_{\Delta_g U}. \quad (1)$$

The extension for non-Euclidean embedding space is treated in [19, 20, 21, 22, 11, 18], see also in [24, 23, 5]. Note that we didn't specify the metric yet. If we choose for a metric the first fundamental form of the base, non-flat, manifold then this flow is the intrinsic-explicit analog of the L_2 based harmonic map equation [3]. Both equations describe a **linear operator** that acts on the image function U. One major difference between the Beltrami framework and the harmonic map formulation is the way one chooses the metric. In the harmonic map approach it is treated as an a-priori knowledge which is given beforehand. The metric then is **constant in time**. In the Beltrami framework **the metric is a dynamic variable to be found by minimizing the functional**. Carrying out the calculation one finds the metric to be [19, 20] :

$$(g_{\mu\nu}) = \begin{pmatrix} 1 + U_x^2 & U_x U_y \\ U_x U_y & 1 + U_y^2 \end{pmatrix}. \quad (2)$$

where U denotes the intensity level. In the Beltrami framework, therefor, the manifold of interest, and the metric, is taken to be **the data surface** i.e. the graph of the intensity function. In other words we are interested in the structure of **the section** of the fiber bundle and not in the base manifold. It means that **the metric itself depends on the data**. This is the way non-linearities are introduced in the flow.

This choice of the induced metric gives a simple geometric meaning to the functional as well. It becomes simply the volume of the section (area or length for the two- and one- dimensional cases). It is important for the study below to have the explicit form of the functional for flat domains in the scalar case:

$$S_{\mathrm{scalar}}[I] = \int dx dy \sqrt{g} = \int dx dy \sqrt{1 + \beta^2 ||\nabla I||^2}, \quad (3)$$

where β is the ratio between the distances taken in the spatial and intensity directions. Note that this functional was obtained in the Φ-formulation [8, 12] and it is also equivalent, in the limit $\beta \to \infty$, to the L_1 norm of [16].

The gradient descent flow is

$$U_t = \frac{1}{\sqrt{1 + \beta^2 ||\nabla U||^2}} Div\left(\frac{\beta^2 \nabla U}{\sqrt{1 + \beta^2 ||\nabla U||^2}}\right). \quad (4)$$

3. SCALAR FIELD ON IMPLICIT MANIFOLDS

We treat here the case where we have an n-Dimensional manifold on which a scalar quantity is defined. We describe the manifold by the zero level of a function on $\mathbb{R}^{n+1}$ space i.e. $\Psi(x_1, \ldots, x_{n+1}) = 0$ and we extend the scalar data to $\mathbb{R}^{n+1}$ as well by the function $U(x_1, \ldots, x_{n+1})$. The data manifold is described then as an n-Dimensional manifold embedded in $\mathbb{R}^{n+2}$ given by the intersection of the two implicit (n+1)D hyperplanes: $\Psi(x_1, \ldots, x_{n+1}) = 0$ and $\Phi(x_1, \ldots, x_{n+1}) = x_{n+2} - \beta U(x_1, \ldots, x_{n+1}) = 0$. Note that Ψ does not depend on x_{n+2}. This is not the most general form

because, by the Nash theorem, it is not always true that one can represent an n-Dimensional manifold as a zero set of a function in (n+1) Euclidean space. Nevertheless it is true for 2d surfaces that we treat below, and for most cases of interest in computer vision and computer graphics. We define the $\mathbb{R}^{n+2}$ gradient D and the $\mathbb{R}^{n+1}$ gradient ∇. The functional is simply the volume of this n-Dimensional manifold. Note however that this is the **data manifold** and not the fixed underlying manifold described by Ψ.

We have shown in [1] that the volume of the fiber section can be written as:

$$V = \int \delta(\Psi)\delta(\Phi)||D\Psi||||P_{D\Psi}D\Phi||dx \cdots dx_{n+2}, \quad (5)$$

where $||D\Psi||^2 P_{D\Psi}D\Phi = ||D\Psi||^2 - D\Psi D\Psi^t$, such that $P_{D\Psi}D\Phi$ is the projection of $D\Phi$ on the tangent space to the surface which is defined implicitly by Ψ. Direct computation gives

$$||P_{D\Psi}D\Phi||^2 = ||P_{D\Psi}D(x_{n+2} - \beta U||^2$$
$$= \begin{pmatrix} -\beta\nabla U & 1 \end{pmatrix} \begin{pmatrix} & & & 0 \\ & P_{\nabla\Psi} & & \vdots \\ & & & 0 \\ 0 & \cdots & 0 & 1 \end{pmatrix} \begin{pmatrix} -\beta\nabla U \\ 1 \end{pmatrix}$$
$$= 1 + \beta^2 ||P_{\nabla\Psi}\nabla U||^2. \quad (6)$$

Using also the fact that $||D\Psi|| = ||\nabla\Psi||$ we see that the integrand in Eq. (5) does NOT depend on x_{n+2} and therefor we can do the integration over this variable trivially:

$$V = \int \delta(\Psi)\delta(\Phi)||\nabla\Psi||\sqrt{1 + \beta^2 ||P_{\nabla\Psi}\nabla U||^2}dx \cdots dx_{n+2}$$
$$= \int \delta(\Psi)||\nabla\Psi||\sqrt{1 + \beta^2 ||P_{\nabla\Psi}\nabla U||^2}dx \cdots dx_{n+1} \quad (7)$$

The equation of motion is derived now by a (modified) gradient descent equation

$$u_t = \frac{1}{||\nabla\Psi||\sqrt{1 + \beta^2 ||P_{\nabla\Psi}\nabla U||^2}}\mathrm{Div}\left(\frac{\beta^2 ||\nabla\Psi||P_{\nabla\Psi}\nabla U}{\sqrt{1 + \beta^2 ||P_{\nabla\Psi}\nabla U||^2}}\right)$$

This is the direct generalization of the flow Eq. (4) that we obtained in the previous section for a scalar data field defined over a flat domain.

4. EXAMPLES AND RESULTS

In this section, we first give some implementation details and then illustrate the capabilities of the approach we have developed to regularize noisy signals and images defined on implicit curves and surfaces. Various experimental results have been carried out, but due to space limitations, we just give some figures for illustrations.

4.1. Implementing the regularization of scalar fields on surfaces

We compute the value of $u^n_{i,j,k}$, the value of u in the pixel (i,j,k) at the nth iteration, based on the values of u^{n-1} at the neighboring pixels. First, we compute the vector $\vec{N} \simeq \nabla\Psi$ (this is needed only once), by central differences. Then, for each iteration n, we visit all pixels to compute:

- The gradient, its projection, and g.

- The divergence.

- The actualization of u.

For the gradient $\vec{v}_{i,j,k}^n$ we used backward differences,

$$\vec{v}_{i,j,k}^n = \nabla_+ u_{i,j,k}^n = \begin{pmatrix} u_{i+1,j,k}^n - u_{i,j,k}^n \\ u_{i,j+1,k}^n - u_{i,j,k}^n \\ u_{i,j,k+1}^n - u_{i,j,k}^n \end{pmatrix}$$

its projection on the surface,

$$(P_{\vec{N}}\vec{v})_{i,j,k}^n = \vec{v}_{i,j,k}^n - \frac{\sum_{m=1}^{3} \vec{N}_{i,j,k}[m] \cdot \vec{v}_{i,j,k}^n[m]}{\left\|\vec{N}_{i,j,k}\right\|^2} \vec{N}_{i,j,k}$$

and g,

$$g_{i,j,k}^n = \|\vec{N}_{i,j,k}\|^2 \left(1 + \beta^2 \|(P_{\vec{N}}\vec{v})_{i,j,k}^n\|^2\right),$$

where square brackets represent the component of the vector. To compute the divergence, we use backward differences,

$$\begin{aligned} \nabla_- \cdot \vec{w}_{i,j,k} &= \vec{w}_{i,j,k}[1] - \vec{w}_{i-1,j,k}[1] + \\ &\quad \vec{w}_{i,j,k}[2] - \vec{w}_{i,j-1,k}[2] + \\ &\quad \vec{w}_{i,j,k}[3] - \vec{w}_{i,j,k-1}[3] \end{aligned}$$

We switch forward differences and backward differences to avoid numerical problems. Finally, the flow implementation is:

$$u_{i,j,k}^{n+1} = u_{i,j,k}^n + \Delta t \frac{1}{\sqrt{g_{i,j,k}^n}} \nabla_- \cdot \left(\frac{\beta \|\vec{N}_{i,j,k}\| (P_{\vec{N}}\vec{v})_{i,j,k}^n}{\sqrt{g_{i,j,k}^n}}\right)$$
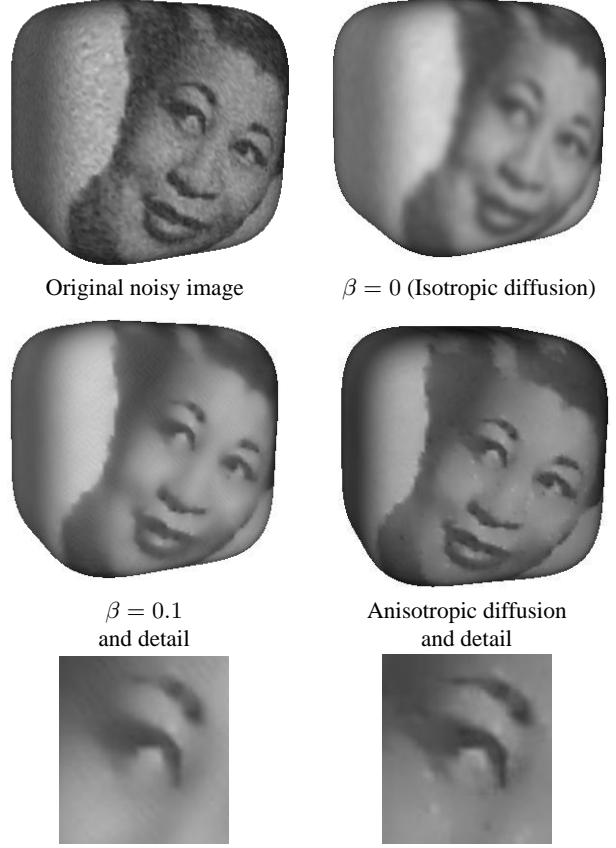
We use a time step $\frac{dt}{\beta}$, adjusted accordingly to section 3.3.

The code is made in C++ using the libraries developed in our lab. For the visualization, we used the marching cubes algorithm [13] to obtain a triangulation from our implicit representation of the surface, and draw the data on this surface. This was made using VTK.

4.2. Examples

We present in this subsection few figures that illustrate the regularization of noisy data on various implicitly defined curves and surfaces. The results are given with various values of the parameter β. Note how the regularization of the data is done isotropically or anisotropically depending on the value of this parameter.

For the Ella photograph, defined in a solid that looks like a quadratic, the image is much bigger (2744000 pixels). The time to compute 20 iterations was almost 3.5 minutes in a 386 sun, 260 MB in RAM. We can see that in strongly noised images like these, where anisotropic regularization treat some noise as part of the image discontinuities (the points under the left eye, for example) the regularization with $\beta = 0.1$ performs better.

Original noisy image $\beta = 0$ (Isotropic diffusion)

$\beta = 0.1$ and detail   Anisotropic diffusion and detail

Finally, for a slice from a cortex (76x100x52) taken from one of our database (Hidden project for anonymous review) it took less than 2 minutes to compute these results.

Original noisy image $\beta = 0$ (Isotropic diffusion)

$\beta = 0.1$ Anisotropic diffusion
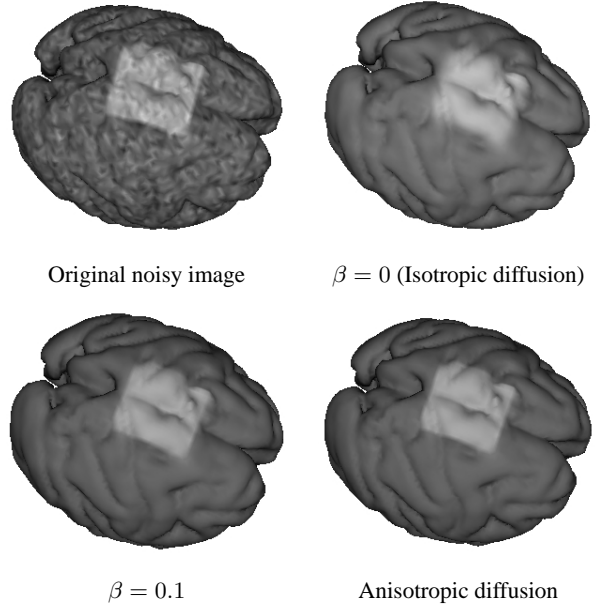
5. SUMMARY AND CONCLUSIONS

In this paper, we have first clarified the link that exists between the the intrinsic Polyakov action of the Beltrami framework and the implicit harmonic energy functional . It is found that although the functionals are basically the same, there are differences in the way various problems are formulated and consequently in the way the functionals are applied.

We used the geometrical understanding of the flat Beltrami flow and generalized it to a denoising flow over implicitly defined curves and surfaces. It is shown that this flow depends on β which encodes the ratio between the data and spatial units. This parameter controls the edge-preserving characteristic of the flow. The Beltrami flow was shown in [2] to act as the linear diffusion (L_2-norm) in the limit $\beta \rightarrow 0$ and to the strongly edge preserving diffusion (L_1-norm) in the limit $\beta \rightarrow \infty$ (up to time scaling).

This work opens interesting perspectives in some important applications such as the inverse EEG-MEG problem. See for instance the work presented in [7] where the authors are interested by localizing cortex activity from EEG/MEG measurements. The PDE associated to the inverse problem includes a regularization term on the implicitly defined surface of the cortex. It could certainly be of interest to apply the implicit Beltrami flow, we developed, to regularize such data defined on implicit cortex surface. It will also be of great interest to compare our result to the methods developed to regularize data defined on triangulated surfaces. We refer the interested reader to our incoming research report where the intrinsic formulation and the derivation of the implicit Beltrami flow from a variational and geometrical points of view are presented (see [1] for details).

6. REFERENCES

[1] N. Sochen and R. Deriche, "The Beltrami flow over Manifolds", INRIA Sophia-Antipolis technical report.

[2] N. Sochen, R. Deriche and L. Lopez-Perez, "The Beltrami flow over Manifolds", submitted to ICCV03.

[3] M. Bertalmío, L. T. Cheng, S. Osher and G. Sapiro, "Variational Problems and Partial Differential Equations on Implicit Surfaces", Journal of Computational Physics 174 (2001) 759-780.

[4] T. Chan and J. Shen, "Variational restoration of non-flat image features: Models and algorithms", SIAM J. Appl. Math., 61 (2000) 1338-1361.

[5] C. Chefd'hotel, D. Tchumperle, R. Deriche, O. Faugeras, "Constrained Flows of Matrix-Valued Functions: Application to Diffusion Tensor Regularization", *Proceedings of 7th European Conference on Computer Vision*, Copenhagen, Denmark, May 2002

[6] L. Cheng, P. Burchard, B. Merriman and S. Osher, "Motion of Curves Constrained on Surfaces Using a Level Set Approach", September 2000 UCLA CAM Technical Report (00-32).

[7] M. Clerc, O. Faugeras, R. Keriven, J. Kybic, T. Papadopoulo, "A level set method for the inverse EEG/MEG problem", Poster No.: 10133, NeuroImage Human Brain Mapping 2002 Meeting

[8] R. Deriche and O. Faugeras, "Les EDP en Traitement des Images et Vision par Ordinateur", INRIA Research Report 2697, Nov. 1995. Also appeared in Traitement du Signal, 13 (6) 1996.

[9] R. Kimmel, "Intrinsic Scale Space for Images on Surfaces: The Geodesic Curvature Flow", *Graphical Models and Image Processing* 59(5) 365-372 1997.

[10] R. Kimmel and R. Malladi and N. Sochen, "Images as Embedding Maps and Minimal Surfaces: Movies, Color, Texture, and Volumetric Medical Images", International Journal of Computer Vision 39(2) (2000) 111-129.

[11] R. Kimmel and N. Sochen, "Orientation Diffusion or How to comb a Porcupine", *Journal of Visual Communication and Image Representation* 13:238-248, 2001.

[12] P. Kornprobst, R. Deriche, and G. Aubert. "Nonlinear operators in image restoration". In Proceedings of the International Conference on Computer Vision and Pattern Recognition - pages 325-331.IEEE Computer Society. San Juan, Puerto Rico, June 1997.

[13] W. E. Lorensen, H. E. Cline, "Marching cubes: A high resolution 3D surface construction algorithm", Computer Graphics, 21(4), pages 163–169, 1987.

[14] F. Memoli and G. Sapiro and S. Osher, "Solving Variational Problems and Partial Differential Equations, Mapping into General Target Manifolds", January 2002 UCLA CAM Technical Report (02-04).

[15] A. M. Polyakov, "Quantum geometry of bosonic strings", *Physics Letters*, **103B** (1981) 207-210.

[16] L. Rudin, S. Osher and E. Fatemi, " Non Linear Total Variation Based Noise Removal Algorithms", *Physica D 60 (1992) 259-268.*

[17] G. Sapiro, "Geometric Partial Differential Equations and Image Analysis", Cambridge University Press, January 2001.

[18] N. Sochen and R. Kimmel, "Stereographic Orientation Diffusion", in proceedings of the 4th Int. Conf. on Scale-Space, Vancouver Canada, October 2001.

[19] N. Sochen and R. Kimmel and R. Malladi, "From high energy physics to low level vision", Report, LBNL, UC Berkeley, LBNL 39243, August, Presented in ONR workshop, UCLA, Sept. 5 1996.

[20] N. Sochen and R. Kimmel and R. Malladi, "A general framework for low level vision", *IEEE Trans. on Image Processing*, 7 (1998) 310-318.

[21] N. Sochen and Y. Y. Zeevi, "Representation of images by surfaces embedded in higher dimensional non-Euclidean space", 4th International Conference on Mathematical Methods for Curves and Surfaces, Lillehamer, Norway, July 1997.

[22] N. Sochen and Y. Y. Zeevi, "Representation of colored images by manifolds embedded in higher dimensional non-Euclidean space", Proc. IEEE ICIP'98, Chicago, 1998.

[23] B. Tang and G. Sapiro and V. Caselles, "Diffusion of General Data on Non-Flat Manifold via Harmonic Map Theory: The Direction Diffusion Case", *International Journal on Computer Vision* 36(2) 149-161, 2000.

[24] D. Tchumperlé and R. Deriche, "Orthonormal Vector Sets Regularization with PDEs and Applications", *International Journal on Computer Vision* 50(3) 237-252 (1992).